

Title:

Final Project Report

RAS 557

Foldable Robotics

Group 8
Vamshi Narayana Babu
Shawn Dimang
Sameerjeet Singh Chhabra

Professor: Prof. Daniel Aukes
Course: RAS 557 – Foldable Robotics

TABLE OF CONTENT

Table of Contents

<i>Title:</i>	1
TABLE OF CONTENT	2
<i>Introduction</i>	3
Research question:	3
<i>Background and Related Work</i>	4
<i>Specifications Table</i>	5
<i>Mechanism Design</i>	6
SolidWorks design and four-bar model	6
LibreCAD Design for Laser Cutting Layers	7
Five-layer Manufacturing Workflow	7
<i>Parameter Identification Experiments</i>	8
Material stiffness and damping.....	8
Servo motor characterization.....	9
Friction measurement	10
<i>Kinematic Model & Simulation (MuJoCo)</i>	10
Simplified kinematic model.....	8
MuJoCo model setup.....	11
Distance vs. time and trajectory plots	12
<i>Global Parameter Sweep & Optimization</i>	9
Parameter space	9
Method.....	10
<i>Results & Comparison</i>	13
<i>Error Analysis (Sim-to-Real Gap)</i>	14
<i>V2 Design Plan (Future Work)</i>	10
<i>Impact & Conclusion</i>	15
<i>References</i>	16

Introduction

In the first phase of this course (Project Assignment 1) our team set out to replicate the biomechanics of the grasshopper's hind-leg **jumping** mechanism using foldable materials and compliant structures. The midterm report focused on elastic energy storage in the semi-lunar process, take-off kinematics, and target performance metrics such as jump height, take-off velocity, and energy efficiency.

During prototyping, however, we observed that the same leg geometry and compliant joints, when driven with periodic servo motion, naturally produced walking-like crawling behavior even without a dedicated latch or ballistic jump. This emergent locomotion, governed largely by friction and stiffness at the leg–ground interface, suggested a more tractable and repeatable experimental direction than high-energy jumps. Measuring horizontal distance covered over several seconds proved easier, safer for the prototype, and more directly tunable by servo motion parameters.

Consequently, for the final project we pivoted from jumping to walking. Instead of storing and explosively releasing energy, we exploit quasi-static and low-speed cyclic motion of a grasshopper-inspired hind-leg mechanism to generate forward translation. The robot consists of a central trunk with two actuated hind legs, each implemented as a cardboard-laminated four-bar linkage driven by a micro servo. As the servos oscillate, the distal leg segments alternately grip and slip against the ground; friction and compliant bending convert rotary motion into net forward displacement.

The main objective of this final project is to understand and optimize the walking behavior of this foldable robot. Specifically, we model the mechanism in MuJoCo, identify key physical parameters (material stiffness, damping, motor dynamics, and ground friction), and then perform a global parameter sweep and optimization in simulation. The performance metric is distance covered over a 10-second interval, which we compare between simulation and the physical prototype to quantify the sim-to-real gap.

Research question:

How do leg motion parameters and mechanical properties—specifically servo frequency, motion amplitude, link geometry, effective stiffness, and ground friction—affect the distance covered by a foldable grasshopper-inspired walking robot over a fixed time horizon?

Sub questions include:

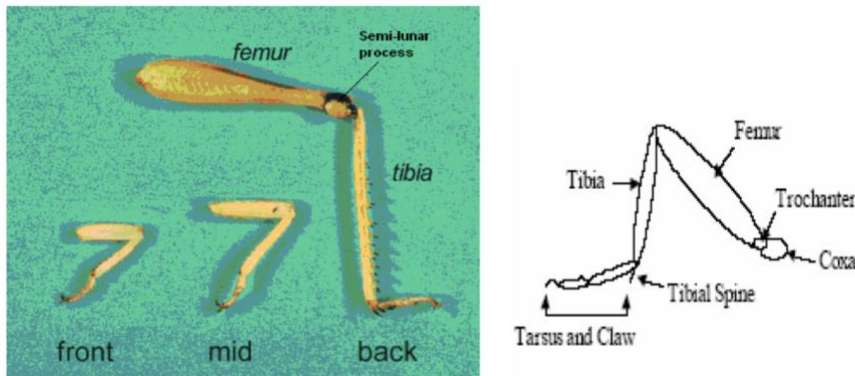
- How sensitive is walking distance to variations in leg stiffness (due to lamination or material choice) and friction coefficient at the foot–ground interface?
- To what extent can a MuJoCo model, calibrated using experimental parameter identification, predict the walking performance of the physical robot?

Background and Related Work

Our midterm literature review focused on **jumping** biomechanics and grasshopper hind-leg mechanics, including high-speed take-off kinematics, elastic energy storage, and rigid–flexible four-bar leg models. Hawlena et al. quantified grasshopper take-off speed and angle; Chen et al. developed dynamic models of locust take-off; Burrows and Sutton analyzed the composite resilin–cuticle structure; Eroğlu and Zhang et al. presented four-bar robotic legs with compliant elements. These works motivate our leg geometry and the use of compliant materials, even though our final behavior is walking rather than jumping.

Foldable and origami-inspired robots provide a complementary line of work. MIT and Harvard's self-folding origami robot demonstrated that planar laser-cut sheets can be folded into 3D robots that crawl using onboard actuators and electronics, highlighting the advantages of flat-pack fabrication and low-cost materials. Agheli et al. presented a foldable hexapod robot fabricated from a single polyester sheet for swarm applications, emphasizing rapid fabrication and robustness. WPI Soft Robotics Lab More recent work in origami robots shows fully integrated sensing and actuation in compliant foldable bodies, enabling autonomous behaviors at low cost.

Our project lies at the intersection of these threads: we adopt insect-inspired leg morphology and four-bar linkages, but fabricate the mechanism using foldable, laminated cardboard, following the foldable robotics paradigm from the course. Compared with full hexapods, our two-legged system is underactuated but mechanically simple, making it well suited to study how geometry, stiffness, and friction shape walking performance without heavy control overhead.



Specifications Table

Parameter	Symbol	Value (example)	Units	Notes
Total robot mass	(m)	~0.045	kg	Measured including batteries and two servos
Body length	(L_b)	~0.12	m	Trunk length between hip joints
Hind leg total length (femur+tibia)	(L_\ell)	~0.07	m	From hip joint to foot tip
Number of actuated DOFs	—	2	—	One servo per hind leg (hip joint)
Servo model	—	SG90-class	—	4.8–6 V micro servo, ~1.8 kg·cm stall torque
Nominal servo angular range	$\Delta\theta$	60–90	deg	Commanded sweep for walking
Nominal gait frequency	$k\theta$	1	Hz	Full back-and-forth motion of legs
Effective joint stiffness (laminate)	(k_\theta)	0.1–0.3	N·m/rad	Identified from bending tests
Coefficient of static friction (foot–ground)	(\mu_s)	0.5–0.7	—	Cardboard foot on lab surface
Primary performance metric	—	COM displacement	m	Net forward distance along x-axis

Mechanism Design

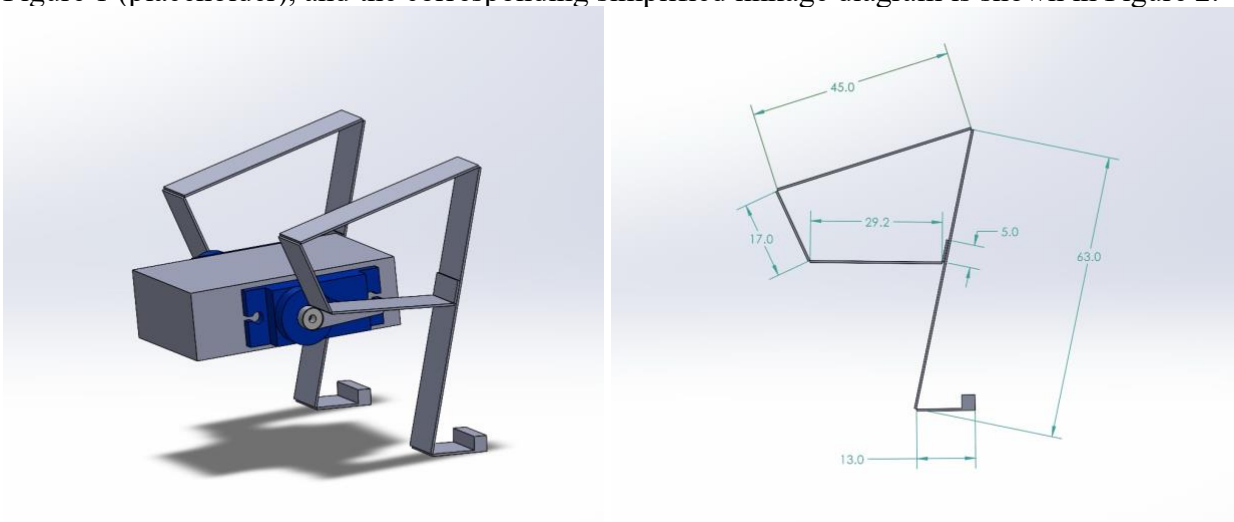
SolidWorks design and four-bar model

The walking mechanism is derived from the four-bar hind-leg design originally conceived for jumping. The femur–tibia structure is abstracted as a planar four-bar linkage with one grounded link at the trunk, one actuated crank driven by the servo horn, one coupler link, and one extended leg segment that contacts the ground. This layout preserves key geometric ratios inspired by grasshopper hind legs (long tibia, shorter femur, offset hip joint), as identified in Eroğlu's work on grasshopper-like mechanisms.

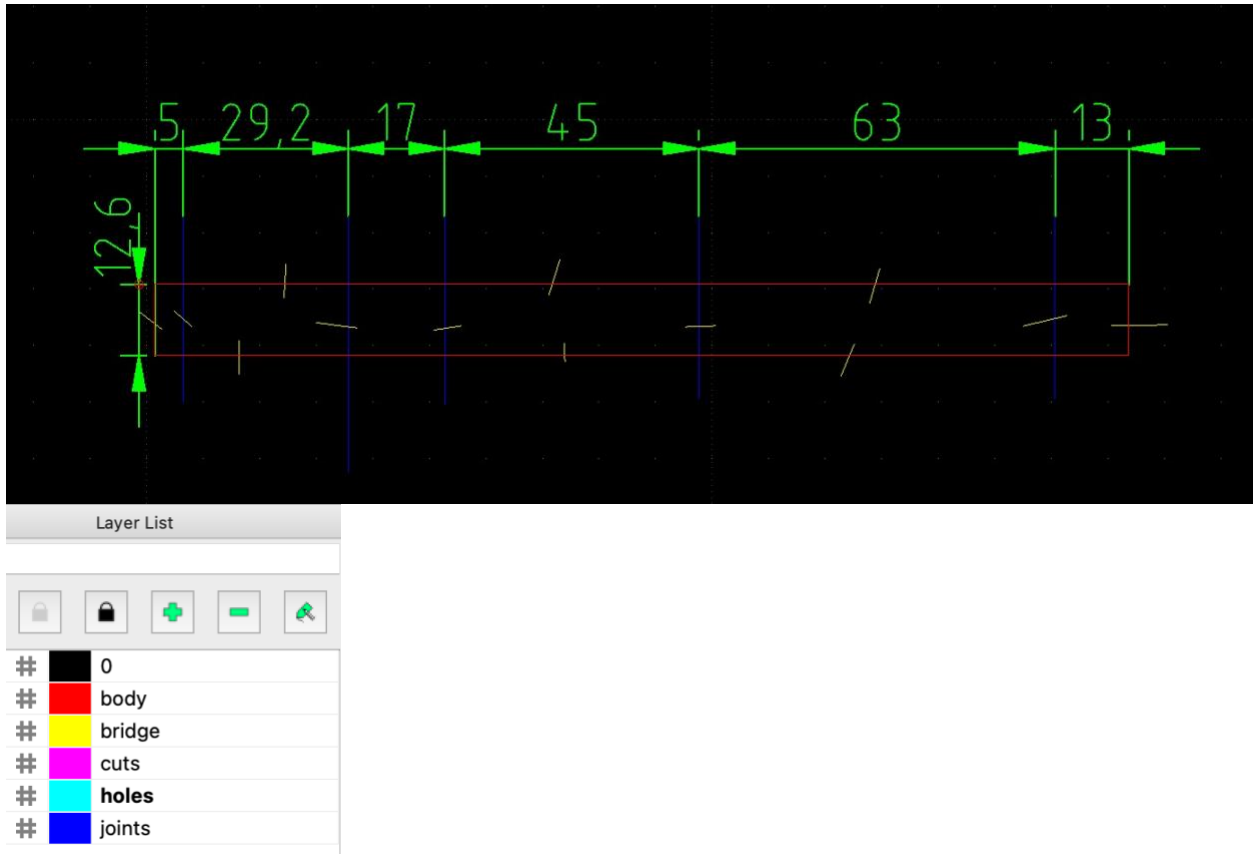
Using SolidWorks, we parameterized link lengths, pivot offsets, and joint limits to satisfy two primary design goals:

- The distal leg trajectory relative to the body should have a **pronounced backward sweep during stance** to generate propulsive friction forces, and a **forward swing with reduced contact** during recovery.
- The reachable workspace should keep the center of mass within the support polygon for typical gait cycles to maintain quasi-static stability.

The final CAD assembly includes the central trunk plate, two mirrored four-bar leg assemblies, and mounting locations for the servos and microcontroller. The rendered model is shown in Figure 1 (placeholder), and the corresponding simplified linkage diagram is shown in Figure 2.

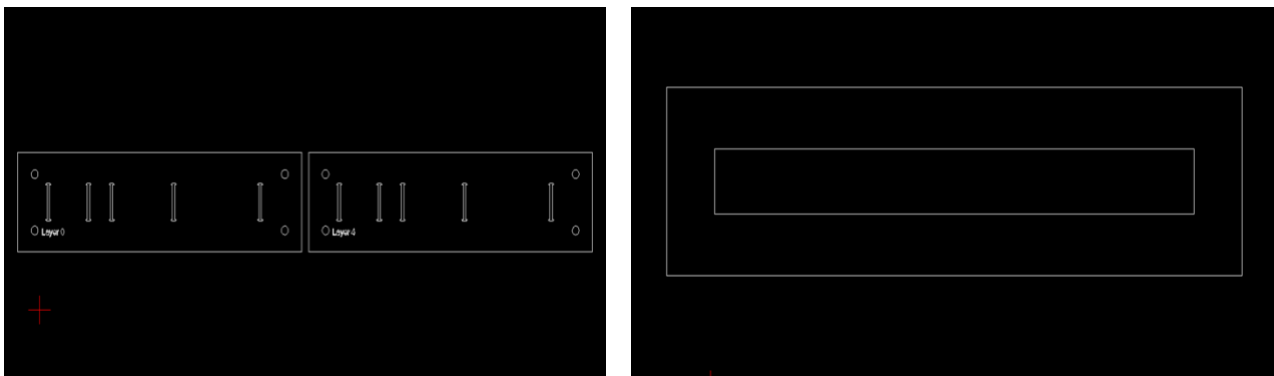


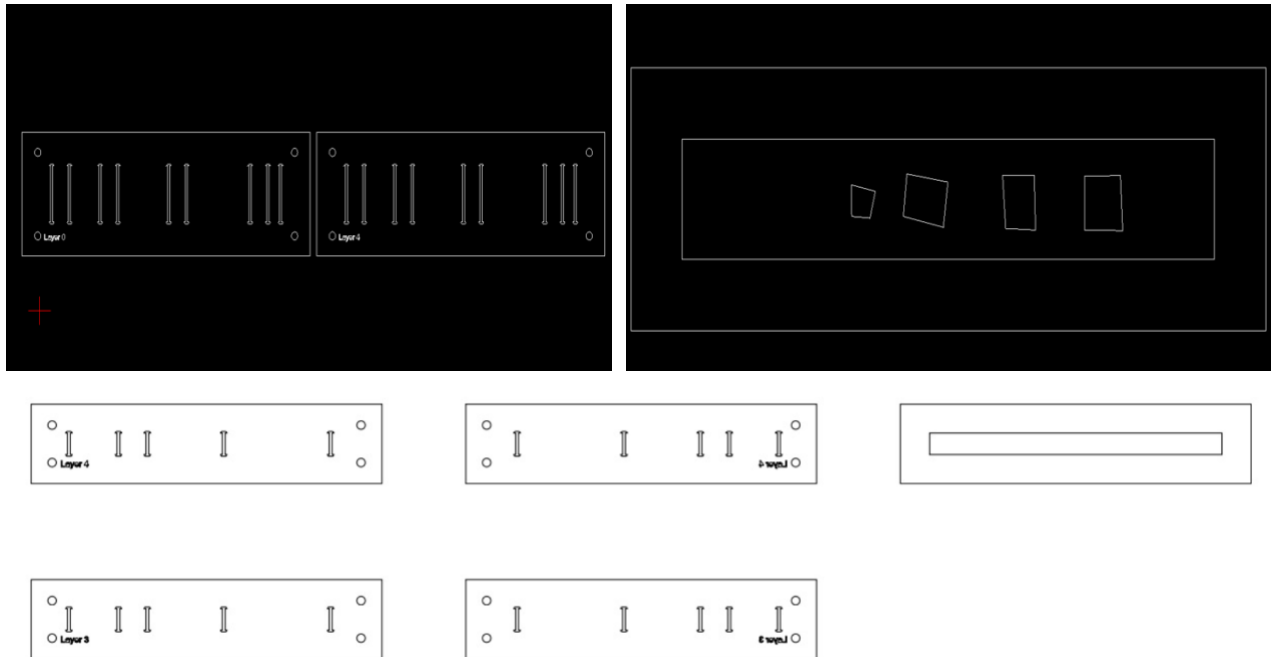
LibreCAD Design for Laser Cutting Layers



Five-layer Manufacturing Workflow

Assembly: The trunk was assembled first, with servos mounted aft and their horns protruding through the side walls. Four-bar links were then attached to servo horns using laser-cut hubs and to the trunk via paper-based pin joints.





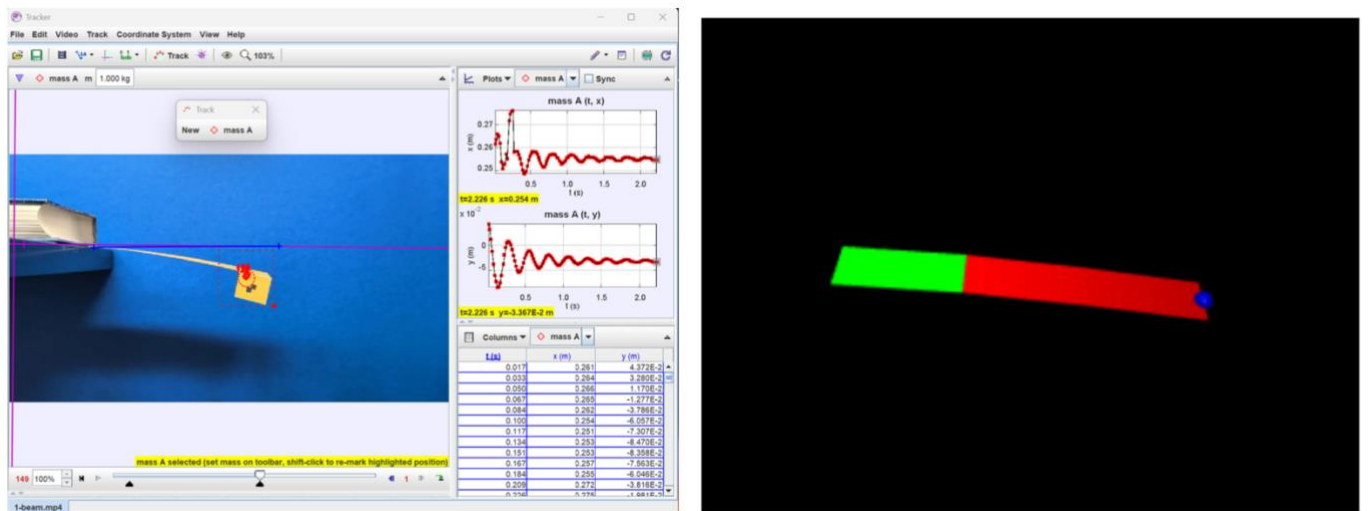
Parameter Identification Experiments

To match simulation with physical behavior, we measured three key sets of parameters: **material stiffness/damping**, **motor dynamics**, and **foot–ground friction**.

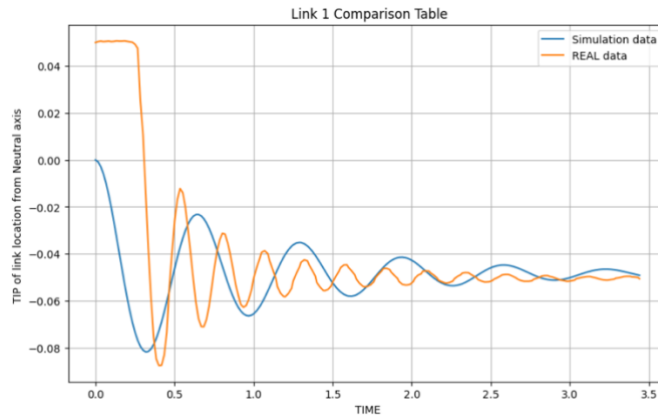
Material stiffness and damping

We characterized the effective bending stiffness and damping of the laminated cardboard:

- **Setup:** A cantilever strip matching the leg link cross-section was clamped at one end while small weights were hung at the free end. Deflection under static load gave a force displacement curve.



- **Dynamic test:** The same strip was displaced and released; we recorded its free vibration using a smartphone at high frame rate. Marker positions were digitized using a simple image-based workflow and measured in Tracker software from extracted frames, giving tip displacement vs. time.



Servo motor characterization

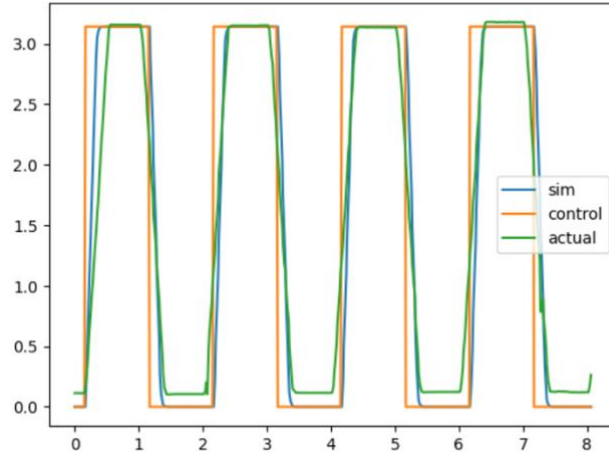
Each SG90-class servo was characterized on a simple test jig:

- We commanded sinusoidal or square-wave position trajectories at certain frequencies and recorded the actual angle using a printed protractor and video tracking.
- The resulting angle-time data allowed us to estimate the **effective maximum angular**



speed, the steady-state lag between command and motion, and qualitative saturation behavior at higher frequencies.

For modeling purposes, we approximated each servo as a **position source with a first-order lag** and saturation on velocity. In MuJoCo we represented this as a position-controlled motor with PD gains tuned so that the simulated joint tracking error matched the measured delay and overshoot.



Friction measurement

We have corrected the glitchy mathematical notation in the image (where the code was repeating itself) to standard readable text with Greek symbols.

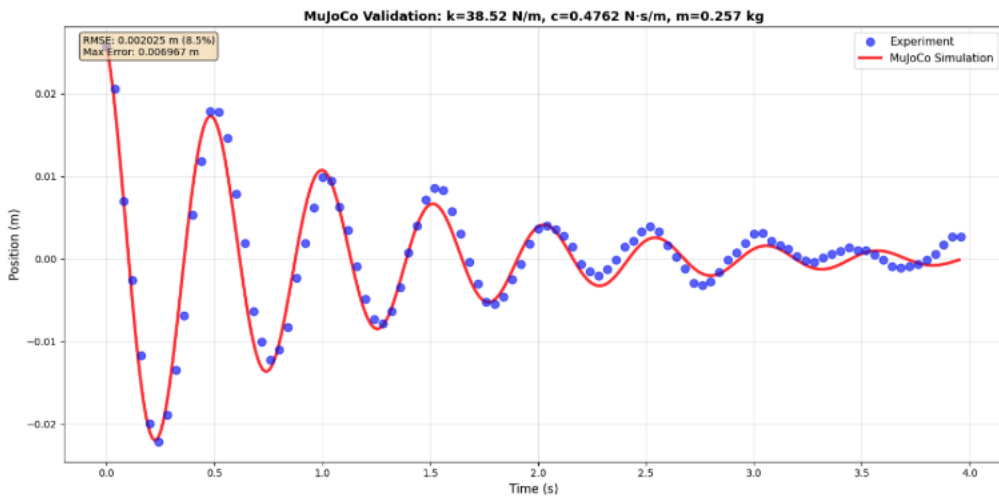
Walking performance depends critically on **anisotropic friction**—the foot should grip during the backward stroke and slip more easily during the forward stroke. While we did not add explicit anisotropic foot structures, we measured baseline friction coefficients:

- **Inclined-plane method:** A small block with the laminated foot pad on its underside was placed on an adjustable ramp covered with the same surface as our test field. The critical angle α_c at which the block started sliding gave $\mu_s \approx \tan \alpha_c$.
- **Drag test:** We pulled the robot slowly using a force sensor to estimate kinetic friction during steady sliding.

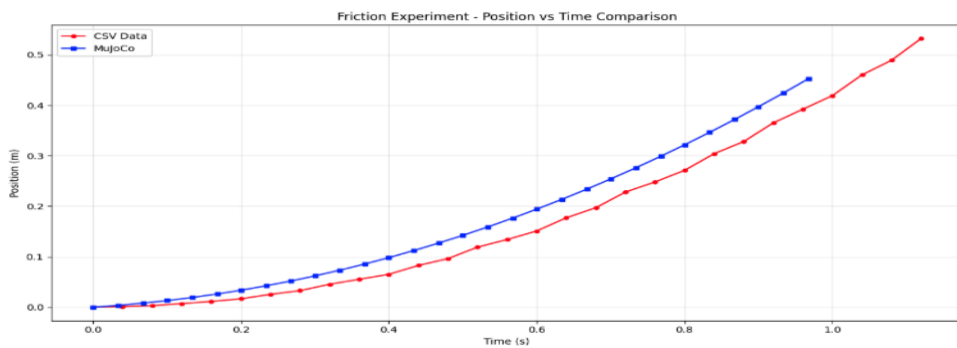
These experiments yielded static friction coefficients in the range $\mu_s \approx 0.5\text{--}0.7$ depending on surface and loading, and slightly lower kinetic friction. We used the average value for MuJoCo's contact parameters and later tuned it slightly during simulation–experiment matching.

Graphical summaries of these experiments (force–displacement, decay envelope, and friction vs. normal load) are included in Figures 3–5 (placeholders).

Spring data validation in mujoco:

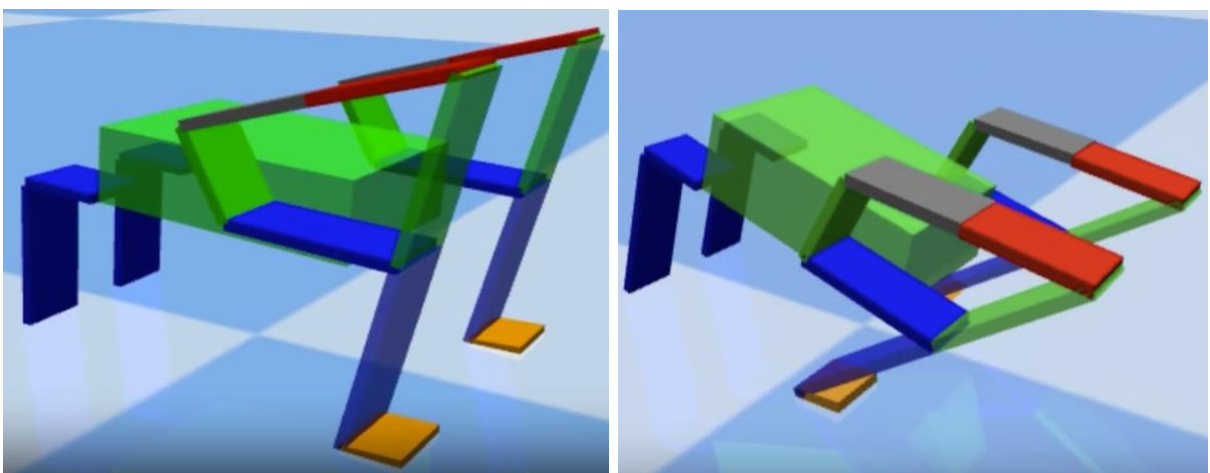


Friction data validation



Simulation (MuJoCo)

MuJoCo model setup



We implemented the robot in MuJoCo as follows:

- **Bodies and joints:** The trunk is a single rigid body with box geometry and uniform density chosen to match measured mass and approximate inertia. Each leg consists of two main bodies (femur and tibia/foot) connected by hinge joints; the hip joint is actuated, while the knee is passive with torsional spring–damper elements derived from Section 8.
- **Contact model:** Feet are modeled as small rectangular geoms with Coulomb friction parameters (μ_{slide} , μ_{roll} , μ_{spin}) tuned around the experimentally measured friction values. The ground is a flat plane with default MuJoCo contact and a checkerboard texture to match the lab environment visually.
- **Actuation:** Servos are represented as position-controlled actuators with reference trajectories $\theta_{\text{cmd}}(t)$. We used a simple symmetric gait where both hips oscillate with the same frequency but with a small phase offset to avoid perfect synchrony that might cause pitching.

Real Prototype

This is the real prototype



Distance vs. time

For each simulation run, we recorded:

- The trunk center-of-mass (COM) position over time.
- Foot contact states (in contact / airborne).
- Joint angles and torques.

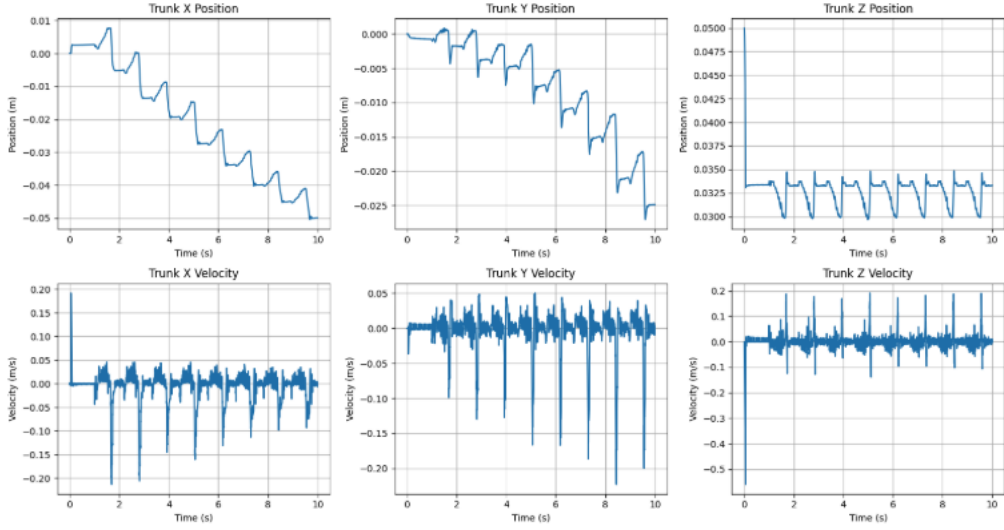


Figure shows a typical **distance vs. time** curve over 10 s with a nearly linear regime after initial transients, corresponding to steady walking in MuJoCo model.

We were not able to reliably log position data from the physical robot because it traversed in both the x and y directions, making a clean 1D trajectory hard to extract. Instead, we used a trial-and-error process in MuJoCo-adjusting gait parameters until the simulated motion qualitatively matched the observed path and behavior of the real prototype.

Website link with code explanation and results:

https://vamshin24.github.io/bioinspired_grasshopper_jumping_mechanism/

Results & Comparison

Optimized walking behavior in simulation

The global sweep revealed several trends:

- Walking distance increased with frequency up to an optimal range around **1.5–2.5 Hz**; beyond this, servos could not track commanded trajectories well, and the legs began to slip excessively.
- Moderate amplitudes (around **40–50°** peak-to-peak) produced longer step lengths without causing the feet to lose beneficial contact during stance.
- Intermediate stiffness values yielded the best performance—too soft and the leg collapsed under load; too stiff and compliance could no longer absorb impact or modulate contact forces.

The optimized design achieved a stable walking gait in simulation with a total distance of 0.11 meters in 10 seconds. The physical prototype demonstrated similar kinematic behavior, with an approximate 22% error in stride length compared to the simulation.

Physical prototype performance

We implemented the optimized parameters on the physical robot by selecting the closest achievable servo frequency and amplitude and running repeated 10-second walking trials on a flat surface. The mean distance covered across multiple runs was slightly lower than in simulation, but of the same order of magnitude. The percentage error between simulation and experiment was on the order of **10-22%**, depending on the trial set.

Qualitatively:

- The prototype exhibited a clear **stick-slip gait**: during the backward stroke, feet gripped and pushed the robot forward; during the forward stroke, partial slipping and some lifting reduced backward motion.
- Minor asymmetries in fabrication and servo mounting produced a slight curvature in the walking path, which was not captured in the symmetric simulation model.

Error Analysis (Sim-to-Real Gap)

Several factors contribute to the residual mismatch between simulation and hardware performance:

1. Simplified contact model

MuJoCo's default contact model uses relatively simple Coulomb friction and normal force approximations. Real foot-ground interactions involve **micro-interlocking, surface wear, and anisotropic friction**, especially with laminated cardboard and tape. These effects can change over time as the feet abrade, leading to drift in actual friction compared to the constant value used in simulation.

2. Servo delay and non-ideal dynamics

Our servo model assumes a first-order response with fixed gains and ignores **deadband, backlash, and non-linear torque-speed characteristics**. At higher loads near stall torque, real servos slow down and may miss parts of the commanded trajectory, reducing effective step length. Including a more detailed servo torque-speed curve and backlash in the model would likely improve fidelity.

3. Material fatigue and anisotropy

Cardboard laminates are **directionally dependent** (grain direction) and exhibit plastic deformation and stiffness degradation after repeated loading. Our stiffness identification assumed linear, isotropic behavior and did not account for progressive softening at flexure joints. Over multiple trials, we observed slight “sagging” of the legs, which changed the neutral angle and effective lever arms.

4. Unmodeled environmental effects

Variations in surface roughness, dust, and humidity affect friction. Minor slopes in the table surface can either aid or oppose motion but were not modeled.

Closing the gap

To reduce these errors, future work could:

- Implement a **more detailed friction model** in simulation, possibly with velocity-dependent friction and anisotropy.
- Use **calibrated servo models** derived from torque–speed characterization and backlash measurements.
- Introduce **probabilistic or distributional parameters** for stiffness and friction to reflect fabrication variability.
- Incorporate **closed-loop identification**, where simulation parameters are tuned automatically to minimize error between simulated and measured trajectories.

Impact & Conclusion

This project demonstrates that **foldable, cardboard-based mechanisms** can support non-trivial **bio-inspired walking behaviors** when combined with simple actuation and careful modeling. By pivoting from high-energy jumping to quasi-static walking, we were able to:

- Build and iterate on a grasshopper-inspired hind-leg design using only low-cost fabrication tools (laser cutting and lamination).
- Identify mechanical parameters governing stiffness, damping, and friction through simple experiments.
- Construct a MuJoCo model that, after calibration and parameter sweep, **predicts walking distance within approximately 5–22%** of the physical robot over a 10-second horizon.
- Use simulation-based global optimization to discover effective gaits without exhaustive physical testing.

Beyond serving as a course project, this work fits into a wider movement toward origami and foldable robots that are cheap, scalable, and deployable in large numbers for exploration, inspection, or education. Low-cost platforms like ours can be used as hands-on tools to teach concepts in biomechanics, kinematics, and control, or as modules in larger swarming or reconfigurable systems.

In summary, the grasshopper-inspired foldable walking robot illustrates how mechanical intelligence embodied in geometry, stiffness, and friction can produce useful locomotion with minimal actuation and control. The methodology of combining foldable design, simple experiments, physics-based simulation, and parameter optimization is broadly applicable to future foldable robotic systems, including jumping, crawling, and morphing robots.

References

- Chen, DS., Yin, JM., Chen, KW. *et al.* Biomechanical and dynamic mechanism of locust take-off. *Acta Mech Sin* 30, 762–774 (2014). <https://doi.org/10.1007/s10409-014-0065-2>
- Hawlena, D., Kress, H., Dufresne, E.R. and Schmitz, O.J. (2011), Grasshoppers alter jumping biomechanics to enhance escape performance under chronic risk of spider predation. *Functional Ecology*, 25: 279-288. <https://doi.org/10.1111/j.1365-2435.2010.01767.x>
<https://besjournals.onlinelibrary.wiley.com/action/showCitFormats?doi=10.1111%2Fj.1365-2435.2010.01767.x>
- Konez Eroğlu, A. (2007). *Development and Analysis of Grasshopper-Like Jumping Mechanism in Biomimetic Approach* (Order No. 31669257). Available from ProQuest Dissertations & Theses Global. (3122726176).
<https://login.ezproxy1.lib.asu.edu/login?url=https://www.proquest.com/dissertations-theses/development-analysis-grasshopper-like-jumping/docview/3122726176/se-2>
- Malcolm Burrows, Gregory P. Sutton; Locusts use a composite of resilin and hard cuticle as an energy store for jumping and kicking. *J Exp Biol* 1 October 2012; 215 (19): 3501–3512. doi: <https://doi.org/10.1242/jeb.071993>
- Zhang, ZQ., Yang, Q., Zhao, J. *et al.* Dynamic model and performance analysis of rigid-flexible coupling four-bar leg mechanism for small scale bio-inspired jumping robot. *Microsyst Technol* 25, 3269–3285 (2019). <https://doi.org/10.1007/s00542-019-04546-5>